THE EFFECT OF IMAGE POINT DENSITY ON PHOTO-VARIANT AND PHOTO-INVARIANT BUNDLE ADJUSTMENT

W. Faig & K. Owolabi
Department of Surveying Engineering
University of New Brunswick
P.O. Box 4400
Fredericton, New Brunswick, Canada
Commission III

ABSTRACT

Various additional parameter sets are available for compensating systematic errors in bundle adjustment. However, the compensating powers of these models in the face of varying image densities and distributions have not hitherto been established. This paper compares the effectiveness of various additional parameter models in both photo-variant and photo-invariant bundle adjustment.

1. INTRODUCTION

The occurence of errors in our measurements is a natural phenomenon. The importance of their removal from the data, before making a decision based on these, has been emphasized for several centuries. In particular, the importance of identification and elimination of systematic errors in photogrammetric measurement has been stressed as a precondition for photogrammetry to perform reliably as a technique for high precision point determination. One major stumbling block to achieving this goal is the incomplete knowledge of systematic errors affecting the image coordinates.

The sources of some of these systematic errors in classical photogrammetry have been identified to include: film deformation, lens distortion, atmospheric refraction and other anomalous distortions. Significant contributions in their mathematical modelling have been made, among others, by Saastamoinen (1972, 1973) and Schut (1969) on refraction, Brown (1966, 1968) and Washer (1963) on lens distortion, and Ziemann (1968, 1971a, 1971b) on film deformation.

In the beginning, mathematical correction models were used for data refinement prior to entering a photogrammetric block adjustment. With systematic errors thought to have been adequately modelled and computationally accounted for, the disagreement in the results of theoretical and empirical studies among block adjustment procedures led to the hypothesis of existence of residual systematic image errors yet unaccounted for. This led to the concept of additional parameters in bundle adjustment as we know it today.

Individual research results (e.g. Bauer and Mueller, 1972; Bauer, 1974; Moniwa, 1977; El-Hakim and Faig, 1977; El-Hakim, 1979; Ackermann, 1980) encouraged the International Society of Photogrammetry and Remote Sensing to create a working group under Commission III for the period 1980-1984 to "unify the approaches for the identification and elimination of systematic errors" (Kilpela, 1984). The report of the activities of the working group was outlined by Ackermann (1984) where it was noted that improvement in accuracy of bundle adjustment can be achieved through the use of additional parameters. Inspite of the accuracy improvement, there is still no definite pattern as to the "extent the method is effective or how the success depends on overlap, control, density of points or on the particular set of parameters" (Ackermann, 1984). The motivation for this paper was based on this comment, the objective of which is to compare the compensating powers of various additional parameter models in both photo-variant and photo-invariant bundle adjustment when varying image densities and control point patterns.

2. CLASSIFICATION OF ADDITIONAL PARAMETERS

The basic mathematical model for a self-calibrating bundle adjustment is the extended form of the well-known collinearity equations given by:

$$x - x_o + \Delta_x = c\frac{\Delta N_x}{\Delta D};\ y - y_o + \Delta_y = c\frac{\Delta N_y}{\Delta D} \qquad (1)$$

where:

$\Delta N_x = f(\omega,\phi,k,X_e,Y_e,Z_e,X_s,Y_s,Z_s)$

$\Delta N_y = g(\omega,\phi,k,X_e,Y_e,Z_e,X_s,Y_s,Z_s)$

$\Delta D = h(\omega,\phi,k,X_e,Y_e,Z_e,X_s,Y_s,Z_s)$

$\omega,\phi,k,X_e,Y_e,Z_e$ = exterior orientation elements

X_s,Y_s,Z_s = object space coordinates

c,x_o,y_o = basic interior orientation elements

Δ_x,Δ_y = additional parameters

x,y = photo coordinates.

Conceptually, Δ_x and Δ_y should consist of the sum of the mathematically modelled distortions. However, there are different schools of thought on the form of the structure of the additional parameter model, leading to as many as eighteen additional parameter sets available in the literature (see Table 1).

Generally, additional parameter models can be seen as consisting of two major groups. The first group consists of those sets whose terms can be identified with the mathematical models already developed for the known distortions. The second group does not try to account for individual physical causes; rather it uses an expression such as general polynomial or harmonic function to model the combined effect of all possible systematic image errors in the functional model. Some parameter sets can be identified to be a combination of these two groups. A close look at all the additional parameter sets found in the literature produced the following classification (see Table 1):

Class A: modelling known physical causes
Class B: modelling effects by polynomial functions
Class C: modelling effects by trigonometric and/or harmonic functions
Class AB: combination of classes A and B
Class BC: combination of classes B and C
Class AC: combination of classes A and C

Table 1: A Collection of Additional Parameter Models

Name	Class	# of Parameters	References/Remarks
ANO	-	-	No additional Parameters
BRO	AB	18	Brown (1976), Set A of WG III/3
EBN	B	12	Ebner (1976), Set B of WG III/3
ELF	C	20	El-Hakim and Faig (1977), Set C of WG III/3
ELZ	C	14	Ziemann and El-Hakim (1985)
GRA	B	12	Grun (1978), Set F of WG III/3
GRB	B	7	Grun (1978). Set D of WG III/3
GRC	B	10	Grun (1978), Set E of WG III/3
GRD	B	14	Grun (1978), Set G of WF III/3
GRE	B	44	Grun (1978), Set H of WG III/3
JAC	BC	20	Jacobsen (1982), Set J of WG III/3
KIL	AB	7	Kilpela (1980)
KOJ	BC	9	Juhl et al. (1982)
KOL	BC	9	Kolbl (1975)
MAU	B	14	Kupfer and Mauelshagen (1982)
MOA	A	7	Moniwa (1977)
MOB	C	11	Moniwa (1981)
MUR	A	9	Murai et al. (1984)
SCH	B	14	Schut (1979)

3. GENERALIZED MATHEMATICAL MODEL FOR BUNDLE SOLUTION

Using the concept of partitioning of parameters, equation (1) forms the core of a mathematical model for a generalized bundle solution. The generalized mathematical model is composed of the following submodels:

$$\ell_p = f_p(x^i, x^e, x^s), P_p;\ \ell_g = f_g(x^e, x^n, x^s), P_g \qquad (2a,b)$$

$$\ell_{x^1} = x^1, P_{x^i};\ \ell_{x^e} = x^e, P_{x^e};\ \ell_{x^n} = x^n, P_{x^n};\ \ell_{x^s} = x^s, P_{x^s} \qquad (2c,d,e,f)$$

Equation (2a) models the extended collinearity equations (1) where ℓ_p is a vector of observed photo coordinates, x^1 is a vector of interior orientation elements including additional parameters, x^e is a vector of exterior orientation elements and x^s is a vector of object space coordinates.

Equation (2b) models all the non-photogrammetric observations that are expressible in terms of either x^e or x^s or both including possible nuisance parameters, x^n, in such observations. Equations (2c - 2f) represent possible admission of observations on the unknown parameters with their respective weight matrices P.

Equations (2) have been developed into an algorithm and a software in which each additional parameter set shown in Table 1 is coded as a subroutine. Thus, any desired additional parameter set can be activated in the adjustment through a variable in the input data.

4. INVESTIGATED DATASETS

In order to get a clear picture of how an individual additional parameter set behaves with varying image point densities and control point patterns, and also to determine the behavioural pattern when used in photo-variant and photo-invariant modes, seventeen datasets were created from three different blocks of photographs.

The first block of photographs was simulated with photo-invariant systematic image errors using the procedure and software described in Woolnough (1973). Regular points of 11 x 11 per photograph were used, giving rise to high density image points. A high density control point pattern was also selected. The high density image points were reduced by fifty percent to give medium and low density image points respectively. The high density control point pattern was also reduced by fifty percent and seventy five percent to give rise to medium density and sparse control point patterns respectively. The following datasets, comprising of different combinations of image points and control point patterns, were generated from this block.

1. DSA1 - High density image points with high density control point pattern.
2. DSA2 - High density image points with medium density control point pattern.
3. DSA3 - High density image points with sparse control point pattern.
4. DSB1 - Medium density image points with high density control point pattern.
5. DSB2 - Medium density image points with medium density control point pattern.
6. DSB3 - Medium density image points with sparse control point pattern.
7. DSC1 - Low density image points with high density control point pattern.
8. DSC2 - Low density image points with medium density control point pattern.
9. DSC3 - Low density image points with sparse control point pattern.

The second block of photographs used is the Edmundston block described in El-Hakim et al. (1979). As in the first block, the original observations and control point patterns were designated as high density and were then decimated to give the following datasets:

1. DSD1 - High density image points with high density control point pattern.
2. DSD2 - High density image points with sparse control point pattern.
3. DSE1 - Low density image points with high density control point pattern.
4. DSE2 - Low density image points with sparse control point pattern.

Finally, the third block of photographs was simulated with photo-variant systematic image errors and was decimated to give the following datasets:

1. DSF1 - High density image points with high density control point pattern.
2. DSF2 - High density image points with sparse control point pattern.
3. DSG1 - Low density image points with high density control point pattern.
4. DSG2 - Low density image points with sparse control point pattern.

The above notations with prefix 'DS' and the name identifier in column 1 of Table 1 are utilised in the preparation of the tables and figures to follow.

5. ANALYSIS OF RESULTS AND CONCLUSIONS

The additional parameters were given zero weight in this study, thereby treating them as free unknowns. Correlation coefficients greater than 0.7 were printed. Most parameter sets have a few pairs of unknowns registering correlation coefficients greater than 0.7, but this did not make the solution unstable.

Table 2 shows the RMSE values computed from check points for dataset DSA1 along with the performance ranks for the different parameter sets. This is depicted pictorially in Figures 1a and 1b for plan and height respectively. It can be seen that accuracy improvement was achieved by using additional parameters to compensate for the systematic image errors. However, the degree of improvement in planimetry varies from one percent when parameter set GRA was used to eighty nine percent when parameter set KOL was used, while the degree of improvement in elevation varies from ten percent when parameter set GRA was used to eighty one percent when parameter set ELZ was used. Similar results were obtained from datasets DSA1, DSA2 and DSA3 which have the same image point density but different control point patterns (see Tables 3 and 4; Figures 2 and 3). As expected, the RMSE increases with decrease in density of control points. A close look at the pictorial representation of datasets DSA1, DSA2 and DSA3 shows an emerging pattern. Class B parameter sets performed very poorly in all three cases.

Datasets DSB1, DSB2 and DSB3 and datasets DSC1, DSC2, DSC3 have corresponding control point patterns with datasets DSA1, DSA2, DSA3 but differing image point densities. With the exception of parameter sets of the class B type, other parameter sets continue to show tremendous accuracy improvements relative to the case when no additional parameter set was used (see Tables 5-10 and Figures 4-9). In addition though, decrease in image point densities resulted in increased RMSE values for the corresponding paramater set.

Tables 11-14 show results for the real block. Although, accuracy improvements (6% to 29%) were achieved by using additional parameters, they were not as outstanding as those recorded for the simulated block. It is astonishing that in this block, decreased image point density having the same control point pattern with a higher image point density produced better results (compare Tables 11 and 13). It is suspected that the poor geometry of the block (60% overlap and 20% sidelap) might have contributed to this.

Generally, the polynomial function type of parameter set still performs poorer than others in this block. It is important to mention that parameter sets GRE and JAC which have an exceptionally high number of parameters (44 and 20 respectively) actually distorted the results in some cases (see Figures 13a,b).

The last group of datasets concerns the photo-variant solution for simulated data with close-range characteristics. The size of the scale of photography (1/70) is too large to reflect any significant difference between the performances of individual parameter sets. Nevertheless, it can be seen that class B type of parameter sets performed poorly when compared with the others (see Tables 16-19).

Generally, it can be said that polynomial type functions per se should be avoided in self-calibrating bundle adjustment. Rather, they should be combined with either class A or class C type parameter sets for improved results. Parameter sets with trigonometric terms seem to have the best overall performance on the average. At the moment there is no parameter set that forms a combination of classes A and C. In other words, a parameter set that models known causes with the usual terms and models the effect of as yet undetermined anomalous distortions with trigonometric or harmonic functions. It is suggested that a parameter set which forms such a combination be developed and studied extensively to filter out insignificant parameters in order to avoid the danger of overparameterization. It is suspected that such a parameter set would have a consistent behaviour irrespective of the geometry of the block.

TABLE 2 : RMSE FOR DSA1

NAME	XY(M)	RANK	Z(M)	RANK
ANO	1.7424	19	2.7992	19
BRO	0.2328	2	0.5712	3
EBN	1.3194	15	2.0684	15
ELF	0.5612	10	0.6807	8
ELZ	0.2527	6	0.5371	1
GRA	1.7232	18	2.5041	18
GRB	1.7226	17	2.4598	16
GRC	1.6973	16	2.4601	17
GRD	1.1307	12	1.7027	12
GRE	0.5558	9	0.7302	9
JAC	0.2873	8	0.6647	6
KIL	0.2437	4	0.5929	4
KOJ	0.2510	5	1.0425	10
KOL	0.1993	1	0.5635	2
MAU	1.1307	13	1.7027	13
MOA	0.2626	7	0.6757	7
MOB	0.9847	11	1.4732	11
MUR	0.2434	3	0.5947	5
SCH	1.1572	14	1.7718	14

FIG. 1A: RMSE AT XY CHECK POINTS FOR DATASET DSA1

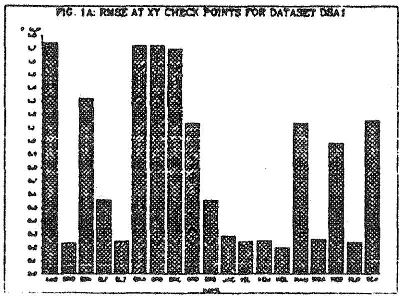

FIG. 1B: RMSE AT Z CHECK POINTS FOR DATASET DSA1

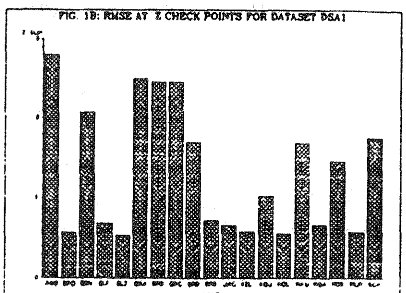

Note: Vertical axis = RMSE value; Horizontal axis = Model name
Model names can be identified with column 1 of the Table

TABLE 3 : RMSE FOR DSA2

NAME	XY(M)	RANK	Z(M)	RANK
ANO	2.2658	19	3.4296	19
BRO	0.2243	3	0.6189	4
EBN	1.6610	15	2.2427	15
ELF	0.6459	10	0.8112	9
ELZ	0.2341	6	0.5535	1
GRA	1.9763	17	2.4920	18
GRB	1.9926	18	2.4601	17
GRC	1.9422	16	2.4527	16
GRD	1.0091	12	1.7682	12
GRE	0.5093	9	0.6724	6
JAC	0.3341	8	0.8437	10
KIL	0.2277	5	0.6065	2
KOJ	0.1498	1	0.7758	8
KOL	0.2263	4	0.6130	3
MAU	1.0091	13	1.7682	13
MOA	0.2667	7	0.7532	7
MOB	0.9619	11	1.3776	11
MUR	0.2181	2	0.6361	5
SCH	1.0429	14	1.8083	14

FIG. 2A: RMSE AT XY CHECK POINTS FOR DATASET DSA2

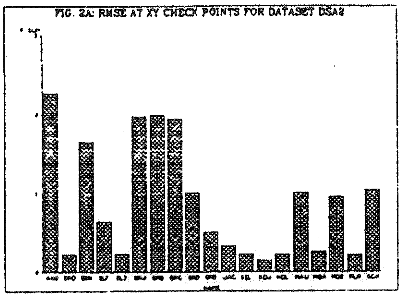

FIG. 2B: RMSE AT Z CHECK POINTS FOR DATASET DSA2

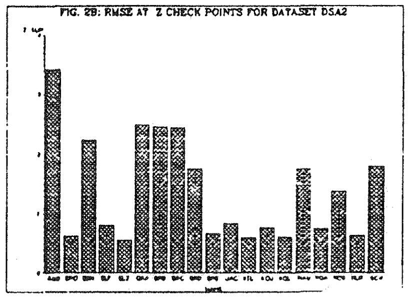

Note: Vertical axis = RMSE value; Horizontal axis = Model name
Model names can be identified with column 1 of the Table

TABLE 4 : RMSE FOR DSA3

NAME	XY(M)	RANK	Z(M)	RANK
ANO	3.0080	19	3.6214	19
BRO	0.4621	6	1.1273	7
EBN	1.7983	15	1.7307	11
ELF	1.0229	10	1.2950	9
ELZ	0.3337	1	0.7101	1
GRA	2.6932	16	2.7846	16
GRB	2.7972	18	2.9100	18
GRC	2.6941	17	2.8131	17
GRD	1.2953	12	1.7319	12
GRE	0.6287	8	0.8432	3
JAC	0.5050	7	1.0513	5
KIL	0.3397	2	0.9156	4
KOJ	0.9437	9	1.4182	10
KOL	1.2170	11	1.7432	14
MAU	1.2953	13	1.7319	13
MOA	0.3676	4	1.0653	6
MOB	0.3602	3	0.7209	2
MUR	0.4389	5	1.1327	8
SCH	1.3357	14	1.8048	15

FIG. 3A: RMSE AT XY CHECK POINTS FOR DATASET DSA3

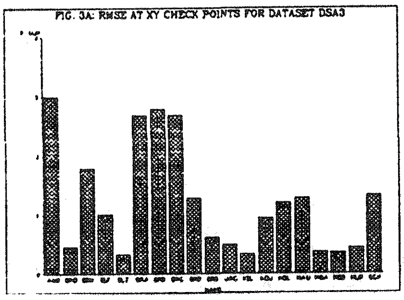

FIG. 3B: RMSE AT Z CHECK POINTS FOR DATASET DSA3

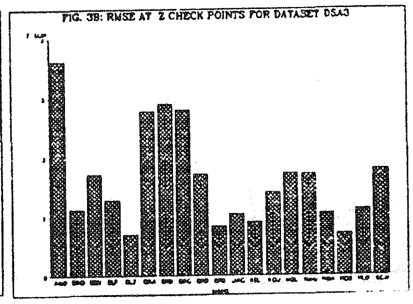

Note: Vertical axis = RMSE value; Horizontal axis = Model name
Model names can be identified with column 1 of the Table

TABLE 5 : RMSE FOR DSB1

NAME	XY(M)	RANK	Z(M)	RANK
ANO	2.1056	16	3.1367	19
BRO	0.1706	6	0.5866	7
EBN	1.2497	12	2.3152	15
ELF	0.4039	8	0.5212	6
ELZ	0.1237	2	0.4557	2
GRA	2.1577	19	2.9601	18
GRB	2.1314	18	2.8733	16
GRC	2.1214	17	2.8761	17
GRD	1.3107	14	2.2407	12
GRE	0.4197	9	0.8868	9
JAC	0.1107	1	0.2646	1
KIL	0.1460	5	0.5015	5
KOJ	0.9980	10	1.6363	10
KOL	0.2488	7	0.7847	8
MAU	1.3107	13	2.2407	13
MOA	0.1313	3	0.4706	3
MOB	1.1380	11	1.7432	11
MUR	0.1336	4	0.4861	4
SCH	1.3344	15	2.2825	14

FIG. 4A: RMSE AT XY CHECK POINTS FOR DATASET DSB1

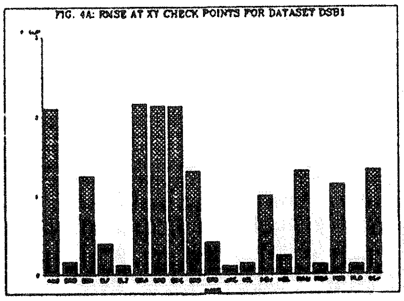

FIG. 4B: RMSE AT Z CHECK POINTS FOR DATASET DSB1

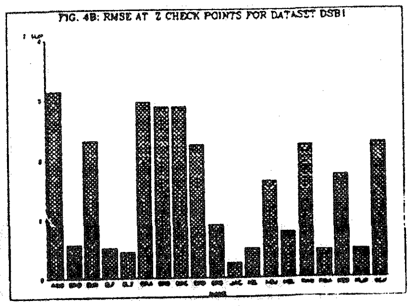

TABLE 6 : RMSE FOR DSB2

NAME	XY(M)	RANK	Z(M)	RANK
ANO	3.2617	19	4.1195	19
BRO	0.2020	5	0.6809	6
EBN	1.7939	11	3.2779	12
ELF	0.6782	9	0.9212	7
ELZ	0.1274	1	0.5316	2
GRA	3.2329	18	3.8397	18
GRB	3.2319	17	3.8189	16
GRC	3.2264	16	3.8359	17
GRD	1.8358	12	3.3008	13
GRE	0.6376	8	1.2632	9
JAC	0.1958	4	0.4400	1
KIL	0.2150	6	0.6244	5
KOJ	1.9175	15	2.1164	10
KOL	0.2933	7	0.9220	8
MAU	1.8358	13	3.3008	14
MOA	0.1616	2	0.5466	3
MOB	1.7880	10	2.4069	11
MUR	0.1623	3	0.5529	4
SCH	1.8480	14	3.3347	15

FIG. 5A: RMSE AT XY CHECK POINTS FOR DATASET DSB2

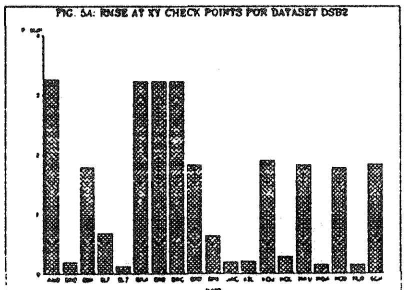

FIG. 6B: RMSE AT Z CHECK POINTS FOR DATASET DSB2

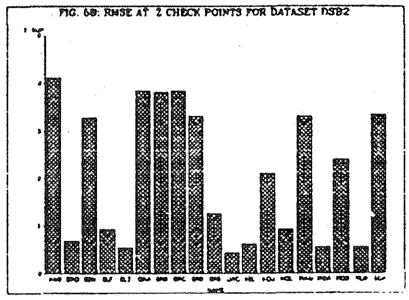

Note: Vertical axis = RMSE value; Horizontal axis = Model name
Model names can be identified with column 1 of the Table

TABLE 7 : RMSE FOR DSB3

NAME	XY(M)	RANK	Z(M)	RANK
ANO	3.0327	19	3.9888	19
BRO	0.2154	2	0.3594	1
EBN	2.5296	15	3.9532	18
ELF	1.1017	10	1.6671	10
ELZ	0.4107	7	0.7131	6
GRA	2.8703	17	3.8041	15
GRB	2.9904	18	3.7732	12
GRC	2.8571	16	3.7932	13
GRD	2.2863	13	3.9196	16
GRE	0.7522	9	1.1394	9
JAC	0.2338	4	0.5498	3
KIL	0.2778	5	0.6121	5
KOJ	0.5018	8	0.9067	8
KOL	0.3790	6	0.8611	7
MAU	2.2863	14	3.9200	17
MOA	0.2171	3	0.5954	4
MOB	1.7604	11	2.4589	11
MUR	0.1827	1	0.4197	2
SCH	2.2855	12	3.7978	14

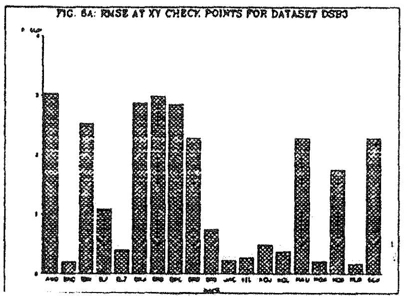
FIG. 6A: RMSE AT XY CHECK POINTS FOR DATASET DSB3

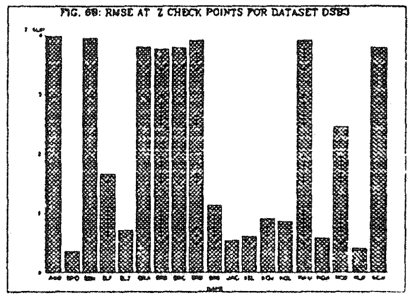
FIG. 6B: RMSE AT Z CHECK POINTS FOR DATASET DSB3

Note: Vertical axis = RMSE value; Horizontal axis = Model name
Model names can be identified with column 1 of the Table

TABLE 8 : RMSE FOR DSC1

NAME	XY(M)	RANK	Z(M)	RANK
ANO	2.2438	19	3.2118	19
BRO	0.1994	6	0.6474	7
EBN	1.2828	15	2.1761	15
ELF	0.2971	8	0.4393	2
ELZ	0.1513	5	0.4971	5
GRA	2.1022	18	2.8513	18
GRB	2.0792	17	2.7689	17
GRC	2.0620	16	2.7574	16
GRD	1.2487	12	2.1091	12
GRE	0.3815	9	0.8635	9
JAC	0.1271	1	0.3011	1
KIL	0.1431	3	0.4901	3
KOJ	0.9177	10	1.6366	10
KOL	0.2593	7	0.8096	8
MAU	1.2487	13	2.1091	13
MOA	0.1426	2	0.4943	4
MOB	1.0860	11	1.7171	11
MUR	0.1465	4	0.5182	6
SCH	1.2753	14	2.1630	14

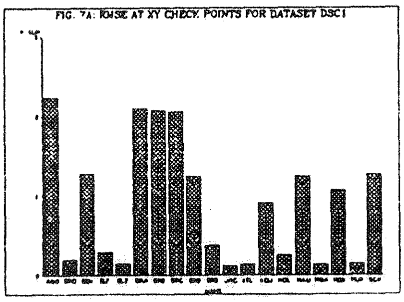
FIG. 7A: RMSE AT XY CHECK POINTS FOR DATASET DSC1

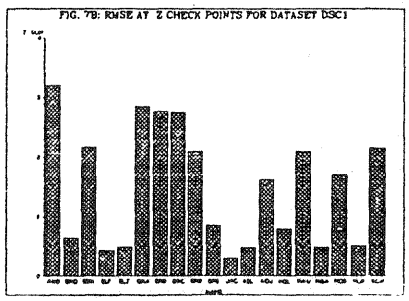
FIG. 7B: RMSE AT Z CHECK POINTS FOR DATASET DSC1

Note: Vertical axis = RMSE value; Horizontal axis = Model name
Model names can be identified with column 1 of the Table

TABLE 9 : RMSE FOR DSC2

NAME	XY(M)	RANK	Z(M)	RANK
ANO	3.2520	19	4.2165	19
BRO	0.3211	6	0.9352	7
EBN	1.8905	14	2.9735	12
ELF	0.4456	8	0.7785	6
ELZ	0.2204	4	0.6973	5
GRA	3.2115	18	3.6863	17
GRB	3.1878	16	3.6175	16
GRC	3.2086	17	3.7101	18
GRD	1.8081	11	3.1463	13
GRE	0.5048	9	1.4785	9
JAC	0.2807	5	0.6422	3
KIL	0.1926	1	0.6379	1
KOJ	2.0026	15	2.2304	10
KOL	0.3458	7	1.0027	8
MAU	1.8081	12	3.1463	14
MOA	0.1937	2	0.6420	2
MOB	1.7206	10	2.4114	11
MUR	0.1939	3	0.6484	4
SCH	1.8290	13	3.2216	15

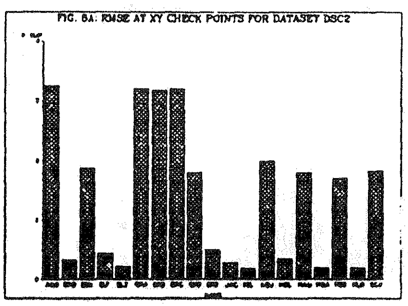
FIG. 8A: RMSE AT XY CHECK POINTS FOR DATASET DSC2

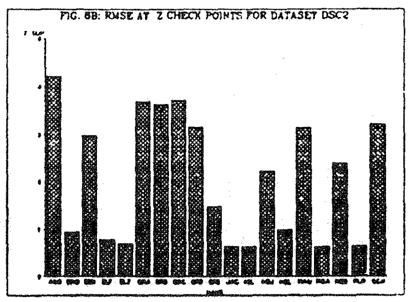
FIG. 8B: RMSE AT Z CHECK POINTS FOR DATASET DSC2

Note: Vertical axis = RMSE value; Horizontal axis = Model name
Model names can be identified with column 1 of the Table

TABLE 10: RMSE FOR DSC3

NAME	XY(M)	RANK	Z(M)	RANK
ANO	2.4222	14	3.2123	11
BRO	0.3078	5	0.4778	1
EBN	2.5065	15	4.0190	14
ELF	0.8048	9	1.6647	9
ELZ	0.3471	7	0.7774	5
GRA	2.8118	16	4.2291	17
GRB	2.8369	18	3.7627	12
GRC	2.8166	17	4.2432	18
GRD	2.3728	12	4.1881	15
GRE	4.1555	19	5.7546	19
JAC	0.3021	4	1.2023	8
KIL	0.2858	3	0.7183	4
KOJ	0.6710	8	1.0384	7
KOL	0.3206	6	1.0311	6
MAU	2.3728	13	4.1881	16
MOA	0.2178	1	0.5737	3
MOB	1.8132	10	2.5459	10
MUR	0.2239	2	0.4929	2
SCH	2.3089	11	4.0100	13

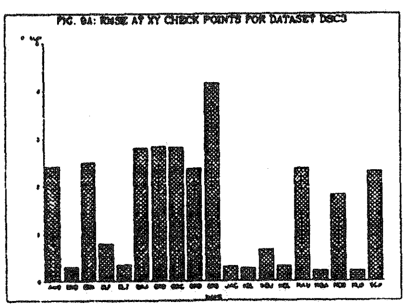
FIG. 9A: RMSE AT XY CHECK POINTS FOR DATASET DSC3

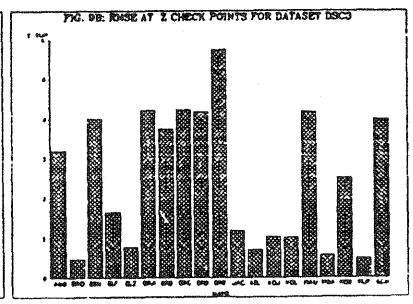
FIG. 9B: RMSE AT Z CHECK POINTS FOR DATASET DSC3

Note: Vertical axis = RMSE value; Horizontal axis = Model name
Model names can be identified with column 1 of the Table

TABLE 11: RMSE FOR DSD1

NAME	XY(M)	RANK	Z(M)	RANK
ANO	0.2018	19	0.2369	19
BRO	0.1684	8	0.1373	6
EBN	0.1848	16	0.2360	18
ELF	0.1636	6	0.1628	9
ELZ	0.1633	5	0.1169	3
GRA	0.1846	15	0.2084	15
GRB	0.1779	12	0.1737	11
GRC	0.1887	18	0.2109	16
GRD	0.1765	10	0.1889	12
GRE	0.1864	17	0.2169	17
JAC	0.1802	14	0.1460	8
KIL	0.1439	1	0.1139	2
KOJ	0.1795	13	0.1242	4
KOL	0.1572	2	0.0934	1
MAU	0.1765	11	0.1889	13
MOA	0.1609	4	0.1345	5
MOB	0.1655	7	0.1708	10
MUR	0.1606	3	0.1451	7
SCH	0.1728	9	0.1935	14

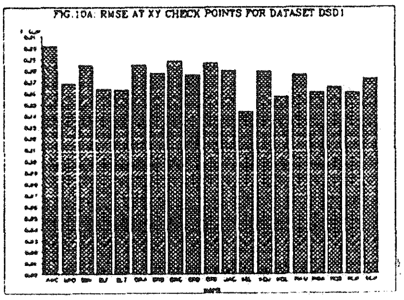
FIG.10A: RMSE AT XY CHECK POINTS FOR DATASET DSD1

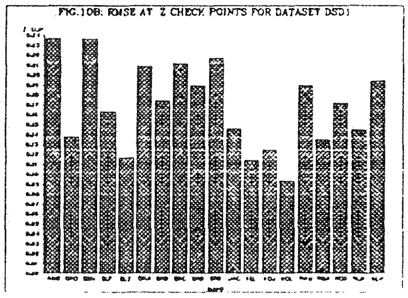
FIG.10B: RMSE AT Z CHECK POINTS FOR DATASET DSD1

Note: Vertical axis = RMSE value; Horizontal axis = Model name
Model names can be identified with column 1 of the Table

TABLE 12: RMSE FOR DSD2

NAME	XY(M)	RANK	Z(M)	RANK
ANO	0.2893	19	0.3015	19
BRO	0.1725	7	0.2002	10
EBN	0.1897	14	0.2470	17
ELF	0.1655	6	0.1495	5
ELZ	0.1850	13	0.1755	7
GRA	0.1939	16	0.2138	12
GRB	0.2055	18	0.1884	8
GRC	0.2013	17	0.2229	16
GRD	0.1793	10	0.2161	13
GRE	0.1911	15	0.3010	18
JAC	0.1727	8	0.2107	11
KIL	0.1449	1	0.0978	2
KOJ	0.1814	12	0.1676	6
KOL	0.1652	5	0.0954	1
MAU	0.1793	11	0.2161	14
MOA	0.1556	4	0.1317	4
MOB	0.1550	3	0.1926	9
MUR	0.1529	2	0.1308	3
SCH	0.1731	9	0.2168	15

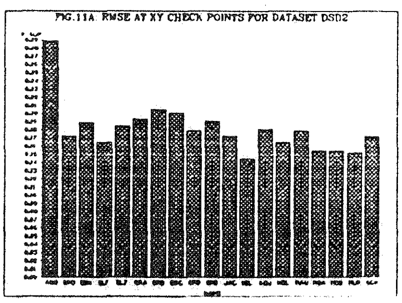
FIG.11A: RMSE AT XY CHECK POINTS FOR DATASET DSD2

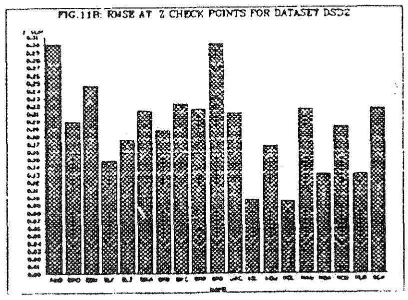
FIG.11B: RMSE AT Z CHECK POINTS FOR DATASET DSD2

Note: Vertical axis = RMSE value; Horizontal axis = Model name
Model names can be identified with column 1 of the Table

TABLE 13: RMSE FOR DSE1

NAME	XY(M)	RANK	Z(M)	RANK
ANO	0.1807	19	0.3466	19
BRO	0.1098	2	0.1286	1
EBN	0.1573	17	0.2627	18
ELF	0.1224	6	0.1901	8
ELZ	0.1212	4	0.1433	2
GRA	0.1447	14	0.2137	14
GRB	0.1481	15	0.2272	15
GRC	0.1522	16	0.2301	16
GRD	0.1327	10	0.1997	11
GRE	0.1626	18	0.2409	17
JAC	0.1265	8	0.2063	13
KIL	0.1044	1	0.1836	5
KOJ	0.1360	12	0.1731	4
KOL	0.1243	7	0.1702	3
MAU	0.1327	11	0.1997	12
MOA	0.1159	3	0.1888	7
MOB	0.1426	13	0.1928	9
MUR	0.1217	5	0.1936	10
SCH	0.1288	9	0.1839	6

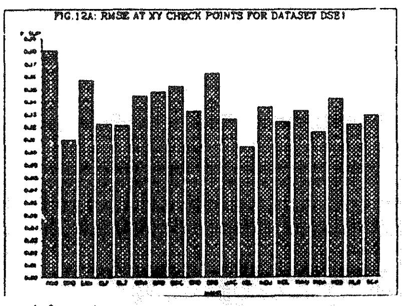
FIG.12A: RMSE AT XY CHECK POINTS FOR DATASET DSE1

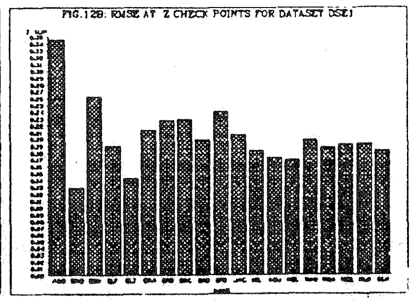
FIG.12B: RMSE AT Z CHECK POINTS FOR DATASET DSE1

Note: Vertical axis = RMSE value; Horizontal axis = Model name
Model names can be identified with column 1 of the Table

TABLE 14: RMSE FOR DSE2

NAME	XY(M)	RANK	Z(M)	RANK
ANO	0.2185	18	0.2395	7
BRO	0.1541	6	0.2191	5
EBN	0.1870	14	0.2804	15
ELF	0.1341	3	0.2156	4
ELZ	0.1792	12	0.2738	13
GRA	0.1791	11	0.2468	8
GRB	0.1844	13	0.2811	16
GRC	0.1966	17	0.2722	12
GRD	0.1737	9	0.2581	9
GRE	0.2901	19	0.3692	17
JAC	0.1951	16	0.4623	19
KIL	0.1081	1	0.1871	1
KOJ	0.1929	15	0.3970	18
KOL	0.1464	5	0.2718	11
MAU	0.1737	10	0.2581	10
MOA	0.1268	2	0.1906	2
MOB	0.1647	7	0.2749	14
MUR	0.1434	4	0.1957	3
SCH	0.1682	8	0.2334	6

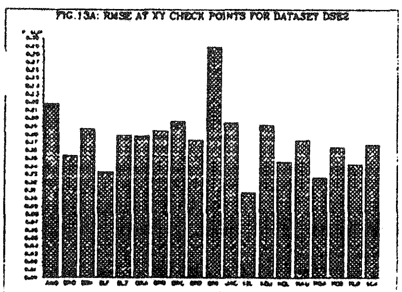
FIG.13A: RMSE AT XY CHECK POINTS FOR DATASET DSE2

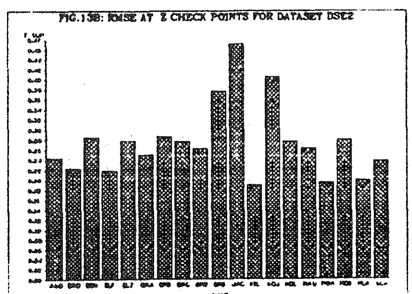
FIG.13B: RMSE AT Z CHECK POINTS FOR DATASET DSE2

Note: Vertical axis = RMSE value; Horizontal axis = Model name
Model names can be identified with column 1 of the Table

TABLE 15: RMSE FOR DSF1

NAME	XY(MM)	RANK	Z(MM)	RANK
ANO	0.0490	19	0.3620	19
BRO	0.0412	7	0.3090	8
EBN	0.0425	17	0.3230	18
ELF	0.0400	4	0.2900	5
ELZ	0.0429	18	0.3120	15
GRA	0.0412	8	0.3090	9
GRB	0.0410	6	0.3130	16
GRC	0.0412	9	0.3090	10
GRD	0.0412	10	0.3090	11
GRE	0.0394	3	0.3160	17
JAC	0.0291	1	0.2300	2
KIL	0.0412	11	0.3070	7
KOJ	0.0389	2	0.2890	3
KOL	0.0423	16	0.3040	6
MAU	0.0412	12	0.3090	12
MOA	0.0421	15	0.3110	14
MOB	0.0400	5	0.2890	4
MUR	0.0412	13	0.1520	1
SCH	0.0412	14	0.3090	13

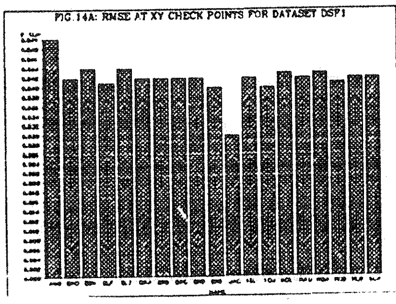
FIG.14A: RMSE AT XY CHECK POINTS FOR DATASET DSF1

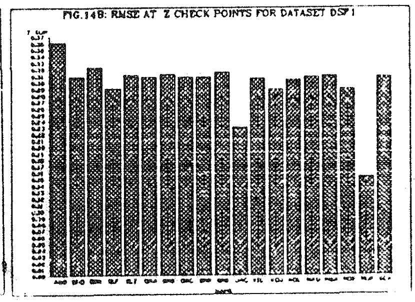
FIG.14B: RMSE AT Z CHECK POINTS FOR DATASET DSF1

Note: Vertical axis = RMSE value; Horizontal axis = Model name
Model names can be identified with column 1 of the Table

TABLE 16: RMSE FOR DSF2

NAME	XY(MM)	RANK	Z(MM)	RANK
ANO	0.0523	19	0.3860	19
BRO	0.0492	8	0.3540	9
EBN	0.0505	17	0.3660	18
ELF	0.0488	6	0.3300	2
ELZ	0.0508	18	0.3530	8
GRA	0.0492	9	0.3540	10
GRB	0.0492	10	0.3560	17
GRC	0.0492	11	0.3540	11
GRD	0.0492	12	0.3540	12
GRE	0.0420	2	0.3300	3
JAC	0.0284	1	0.2290	1
KIL	0.0485	5	0.3490	7
KOJ	0.0461	3	0.3310	4
KOL	0.0478	4	0.3310	5
MAU	0.0492	13	0.3540	13
MOA	0.0499	16	0.3550	16
MOB	0.0488	7	0.3320	6
MUR	0.0492	14	0.3540	14
SCH	0.0492	15	0.3540	15

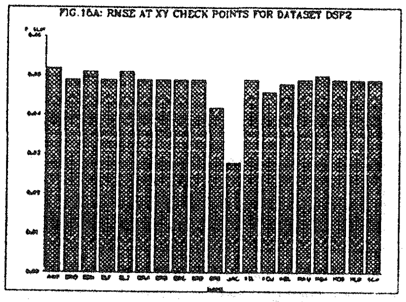
FIG.16A: RMSE AT XY CHECK POINTS FOR DATASET DSF2

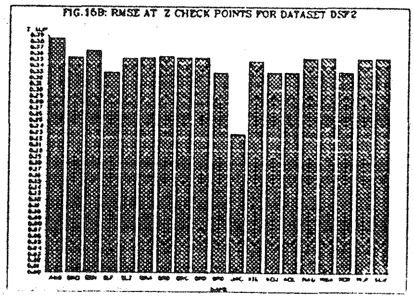
FIG.16B: RMSE AT Z CHECK POINTS FOR DATASET DSF2

Note: Vertical axis = RMSE value; Horizontal axis = Model name
Model names can be identified with column 1 of the Table

TABLE 17: RMSE FOR DSG1

NAME	XY(MM)	RANK	Z(MM)	RANK
ANO	0.0470	18	0.3590	19
BRO	0.0403	7	0.2970	7
EBN	0.0412	16	0.3020	16
ELF	0.0394	3	0.2620	3
ELZ	0.0432	17	0.2960	6
GRA	0.0403	8	0.2970	8
GRB	0.0401	6	0.3010	15
GRC	0.0403	9	0.2970	9
GRD	0.0403	10	0.2970	10
GRE	0.0387	2	0.3120	17
JAC	0.0302	1	0.2120	1
KIL	0.0403	11	0.2950	5
KOJ	0.0398	5	0.2600	2
KOL	0.0492	19	0.3190	18
MAU	0.0403	12	0.2970	11
MOA	0.0403	13	0.2970	12
MOB	0.0394	4	0.2630	4
MUR	0.0403	14	0.2970	13
SCH	0.0403	15	0.2970	14

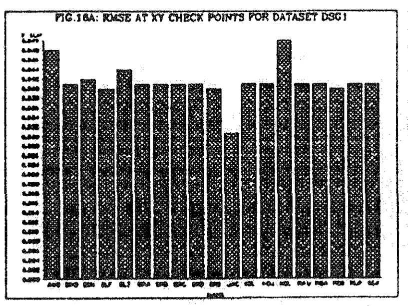
FIG.16A: RMSE AT XY CHECK POINTS FOR DATASET DSG1

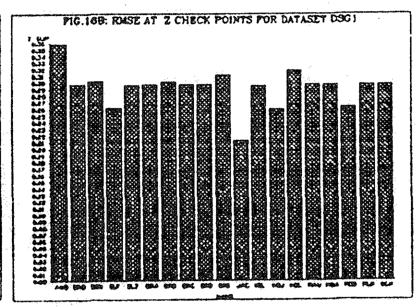
FIG.16B: RMSE AT Z CHECK POINTS FOR DATASET DSG1

Note: Vertical axis = RMSE value; Horizontal axis = Model name
Model names can be identified with column 1 of the Table

TABLE 18: RMSE FOR DSG2

NAME	XY(MM)	RANK	Z(MM)	RANK
ANO	0.0510	17	0.3820	19
BRO	0.0474	6	0.3320	7
EBN	0.0483	16	0.3380	16
ELF	0.0463	4	0.2910	4
ELZ	0.0517	18	0.3390	17
GRA	0.0474	7	0.3320	8
GRB	0.0474	8	0.3340	15
GRC	0.0474	9	0.3320	9
GRD	0.0474	10	0.3320	10
GRE	0.0411	2	0.2190	2
JAC	0.0295	1	0.2070	1
KIL	0.0474	11	0.3280	6
KOJ	0.0452	3	0.2900	3
KOL	0.0545	19	0.3470	18
MAU	0.0474	12	0.3320	11
MOA	0.0474	13	0.3320	12
MOB	0.0463	5	0.2920	5
MUR	0.0474	14	0.3320	13
SCH	0.0474	15	0.3320	14

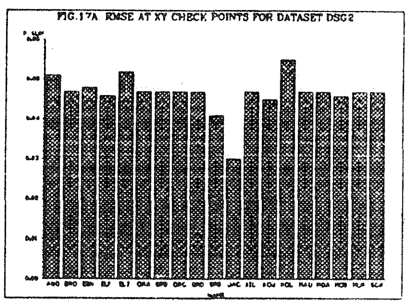
FIG.17A RMSE AT XY CHECK POINTS FOR DATASET DSG2

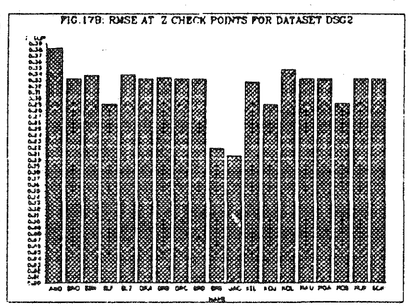
FIG.17B: RMSE AT Z CHECK POINTS FOR DATASET DSG2

Note: Vertical axis = RMSE value; Horizontal axis = Model name
Model names can be identified with column 1 of the Table

REFERENCES

Ackermann, F. (1980). "Block Adjustment with Additional Parameters," *International Archives of Photogrammetry,* Vol. XIV, part 3.

Ackermann, F. (1984). "Report on the Activities of Working Group III/1 During 1980-1984," *International Archives of Photogrammetry and Remote Sensing,* Vol. XXV, part 3.

Bauer, H. (1974). "Bundle Adjustment with Additional Parameters-Pracital Experience" *BUL* 6.

Bauer, H. and J. Mueller (1972). "Height Accuracy of Block and Bundle Adjustment with Additional Parameters," *International Archives of Photogrammetry,* Vol. XII.

Brown, D.C. (1966). "Decentering Distortion of Lens," *Photogrammetric Engineering,* Vol. 32, No. 3.

Brown, D.C. (1968). "Advanced Methods for the Calibration of Metric Cameras," Final Report, Contract DA-04-009-AC-1457X, U.S. Army Topographic Laboratory, Fort Belvoir, VA.

Brown, D.C. (1976). "The Bundle Adjustment-Progress and Prospects," *International Archived of Photogrammetry,* Vol. XIII.

Ebner, H. (1976). "Self-Calibrating Block Adjustment," *International Archives of Photogrammetry,* Vol. XIII.

El-Hakim, S.F. (1979). "Potentials and Limitations of Photogrammetry for Precision Surveying," Technical Report 63, Department of Surveying Engineering, University of New Brunswick.

El-Hakim, S.F. and W. Faig (1977). "Compensation of Systematic Image Errors Using Spherical Harmonics," Proceedings ASP Annual Meeting, Little Rock, Arkansas.

El-Hakim, S.F., H. Moniwa and W. Faig (1979). "Analytical and Semi-Analytical Photogrammetric Programs - Theory and User's Manual," Technical Report 64, Department of Surveying Engineering, University of New Brunswick.

Grun, A. (1978). "Experiences with the Self-calibrating Bundle Adjustment," Proceedings of ACSM-ASP Convention, Washington, D.C.

Grun, A. (1982). "The Accuracy Potential of Modern Bundle Block Adjustment in Aerial Photogrammetry," *Photogrammetric Engineering and Remote Sensing,* Vol. 48, No. 1.

Jacobsen, O. (1982). "Attempt at Obtaining the Best Possible Accuracy in Bundle Block Adjustment," *Photogrammetria,* Vol. 37.

Juhl, J. and O. Brande-Lavridsen (1982). "The AUC Self-Calibrating Block Adjustment Methods and its Results from Jamijarvi Test Field," *Photogrammetria,* Vol. 38.

Kilpela, E. (1980). "Compensation of Systematic Errors in Bundle Adjustment," *International Archives of Photogrammetry,* 23, Part B9.

Kilpela, E. (1984). "Report on the Activities of Commission III 1980-1984," *International Archives of Photogrammetry and Remote Sensing,* Vol. XXV, part 3.

Kolbl, O. (1975). "Tangential and Asymmetric Lens Distortion, Determined by Self-Calibration," *Bildmessung und Luftbildwessen,* 43.

Kupfer, G. and L. Mauelshagen (1982). "Correlations and Standard Errors in Bundle Block Adjustment with some Emphasis on Additional Parameters," *Photogrammetria,* Vol. 38.

Moniwa, H. (1977). "Analytical Photogrammetry System with Self Calibration and its Applications," Ph.D. Dissertation, Dept. of Surveying Engineering, University of New Brunswick.

Moniwa, H. (1981). "The Concept of Photo-variant Self-calibration and its Applications in Block Adjustment with Bundles," *Photogrammetria,* Vol. 36.

Murai, S., R. Matsuoka and T. Okuda (1984). "A Study on Analytical Calibration for Non-metric Camera and Accuracy of Three Dimensional Measurement," *International Archives of Photogrammetry and Remote Sensing.* Vol. XXV, part 5.

Saastamoinen, J. (1982). "Local Variations of Photogrammetric Refraction," ASP Proceedings of the Fall Convention, Part I.

Schut, G.H. (1969). "Photogrammetric Refraction," *Photogrammetric Engineering*, Vol. 35, No. 1.

Schut, G.H. (1979). "Selection of Additional Parameters for Bundle Adjustment," *Photogrammetric Engineering,* Vol. 35, No. 1.

Washer, F.E. (1963). "The Precise Evaluation of Lens Distortion," *Photogrammetric Engineering and Remote Sensing,* Vol. 45, No. 9.

Woolnough, D.F. (1973). "A Ficticious Data Generator for Analytical Aerial Triangulation," Technical Report 26, Department of Surveying Engineering, University of New Brunswick, Canada.

Ziemann, H. (1968). "Reseau Photography in Photogrammetry-A Review," AP-PR-39, National Research Council of Canada.

Ziemann, H. (1971a). "Sources of Image Deformation," *Photogrammetric Engineering,* Vol. 37, No. 12.

Ziemann, H. (1971b). "Image Deformation and Method for its Correction," *The Canadian Surveyor,* Vol. 25, No. 4.

Ziemann, H. and S.F. El-Hakim (1985). "System Calibration and Self-calibration Using Fully Controlled Small Blocks," *Photogrammetria,* (in print).